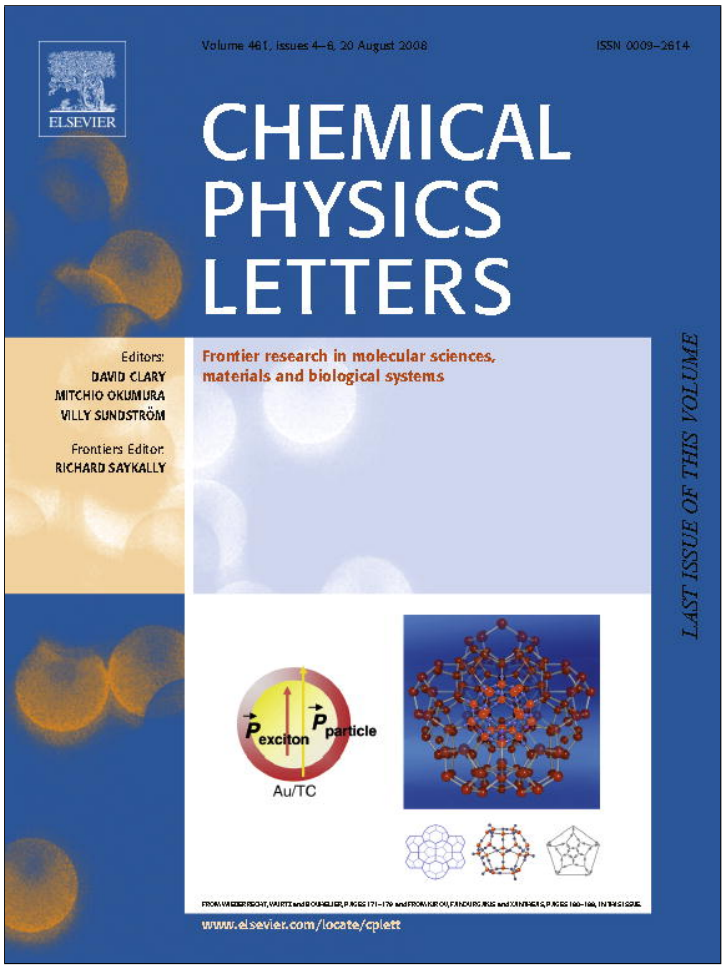

Chemical Physics Letters 461 (2008) 276–279

Contents lists available at ScienceDirect

Chemical Physics Letters

journal homepage: www.elsevier.com/locate/cplett

Enhancement of CO detection in Al doped graphene

Z.M. Ao [a,b], J. Yang [b], S. Li [b,*], Q. Jiang [a,*]

[a] Key Laboratory of Automobile Materials, Ministry of Education, and Department of Materials Science and Engineering, Jilin University, Changchun 130025, China
[b] School of Materials Science and Engineering, The University of New South Wales, NSW 2052, Australia

ARTICLE INFO

Article history:
Received 19 June 2008
In final form 11 July 2008
Available online 16 July 2008

ABSTRACT

A principle of the enhancement of CO adsorption was developed theoretically by using density functional theory through doping Al into graphene. The results show that the Al doped graphene has strong chemisorption of CO molecule by forming Al–CO bond, where CO onto intrinsic graphene remains weak physisorption. Furthermore, the enhancement of CO sensitivity in the Al doped graphene is determined by a large electrical conductivity change after adsorption, where CO absorption leads to increase of electrical conductivity via introducing large amount of shallow acceptor states. Therefore, this newly developed Al doped graphene would be an excellent candidate for sensing CO gas.

Solid-state gas sensors are renowned owing to their high sensitivity, robustness and a wide range of applications as well as low cost and potential for miniaturization [1]. Carbon nanotubes (CNTs) are one of the promising nanoscale molecular sensors used to detect gas molecules with fast response time and high sensitivity at room temperature [2–4]. The semiconducting CNTs are sensitive to variation of electrical conductivity in the presence of gas molecules at the concentration range of ppb (parts per 10^9). However, higher sensitive sensor is desirable for the virtual applications of industrial, environmental and military monitoring.

It was reported that the detectable range and sensitivity of the single wall carbon nanotubes (SWCNTs) can be widened and enhanced substantially through either doping technology or surface engineering [4–6]. For example, SWCNT coated with Pb nanoparticles has high sensitivity to H_2 [5], SnO_2/SWCNTs hybrid material shows an enhanced sensitivity to NO_2 [6]. The high sensitivity of boron doped SWCNT to CO and H_2O absorptions has been also demonstrated [4]. Most recently, Al-cluster and Al doped SWCNT assembly were suggested to be promising systems for novel molecular sensors to NH_3 [7] and CO [8], and the B doped SWCNTs are highly sensitive to the gaseous cyanide and formaldehyde molecules [9]. However, the devices with higher sensitivity to these toxic gases are apparently required for environmental safety issues both in workplaces and residential areas, especially in some industrial and military fields.

Graphene based device may be a solution for ultra-high sensitivity gas sensor for such applications [10–12]. Similar to CNT, the working principle of graphene devices as gas sensors is based on the changes of their electrical conductivity induced by surface adsorbates, which act as either donors or acceptors associated with their chemical natures and preferential adsorption sites [1–3,10]. Graphene is considered to be an excellent sensor material due to its following properties: (1) graphene is a single atomic layer of graphite with surface only, this can maximize the interaction between the surface dopants and adsorbates; (2) graphene has much smaller band gap energy, E_g, than CNT, hence, it has extremely low Johnson noise [13–15], therefore, a little change of carrier concentration can cause a notable variation of electrical conductivity; and (3) graphene has limited crystal defects [13–16], which ensures a low level of excess noise caused by their thermal switching [17]. In this work, we report that the sensitivity of graphene system to CO gas could be enhanced to a higher level based on density functional theory (DFT) calculations, which exceeds by orders of magnitudes the state-of-the-art sensors, through Al doping. This may provide new insight to the development of next generation gas sensors for virtual applications.

All DFT calculations are performed in DMOL^3 code [18,19]. It is widely known that calculations limited at the local density approximation (LDA) overestimate bond energy E_b and underestimate equilibrium distances [20,21]. Thus, a uniform generalized gradient approximation (GGA) with the revised Perdew–Burke–Ernzerhof (PBE) method is used as the exchange correlation function [22]. The DFT semicore pseudopotentials (DSPP) core treatment [23] is implemented for relativistic effects, which replaces core electrons by a single effective potential. To ensure that the results of the calculations are comparable, identical conditions are employed for the isolated CO molecule, the clean Al doped graphene and also the adsorbed graphene system. The k-point is set to $6 \times 6 \times 2$ for all slabs, which brings out the convergence tolerance of energy of 1.0×10^{-5} hartree (1 hartree = 27.2114 eV), and that of maximum force of 0.002 hartree.

In the simulation, three-dimensional periodic boundary condition is taken and C–O bond length is set to l_{C-O} = 1.13 Å, which is consistent with experimental results [24]. For graphene, a single layer 3×3 supercell with a vacuum width of 12 Å above is

* Corresponding authors.
E-mail addresses: sean.li@unsw.edu.au (S. Li), jiangq@jlu.edu.cn (Q. Jiang).

0009-2614/$ - see front matter © 2008 Elsevier B.V. All rights reserved.
doi:10.1016/j.cplett.2008.07.039

constructed, which ensures that the interaction between repeated slabs in a direction normal to the surface is small enough. The variation of energetic results would be within a range of 0.1 eV if the vacuum width is expanded from 12 Å to 15 Å. All atoms are allowed to relax for all energy calculations. The E_b between the CO gas molecule and graphene is defined as

$$E_b = E_{CO+graphite} - (E_{graphite} + E_{CO}) \quad (1)$$

where the subscripts CO + graphene, graphene and CO denote the adsorbed system, isolated graphene and CO molecules, respectively.

For CO adsorption on the intrinsic or Al doped graphene, there are two highly symmetric categories of adsorption configurations: one is CO molecule residing parallel to the graphene surface (Fig. 1a–f), and another is CO molecule residing perpendicular to the graphene surface (Fig. 1g–l). These configurations are similar to that of NO on carbon nanotube [25]. For the Al doped graphene, one Al atom replaces a C atom in the graphene layer with 3×3 supercell as shown in Fig. 2. In this case, the concentration of the doped Al in graphene is 12.5% atomic ration.

To evaluate the interaction between a CO molecule and the intrinsic graphene or Al doped graphene, E_b described in Eq. (1)

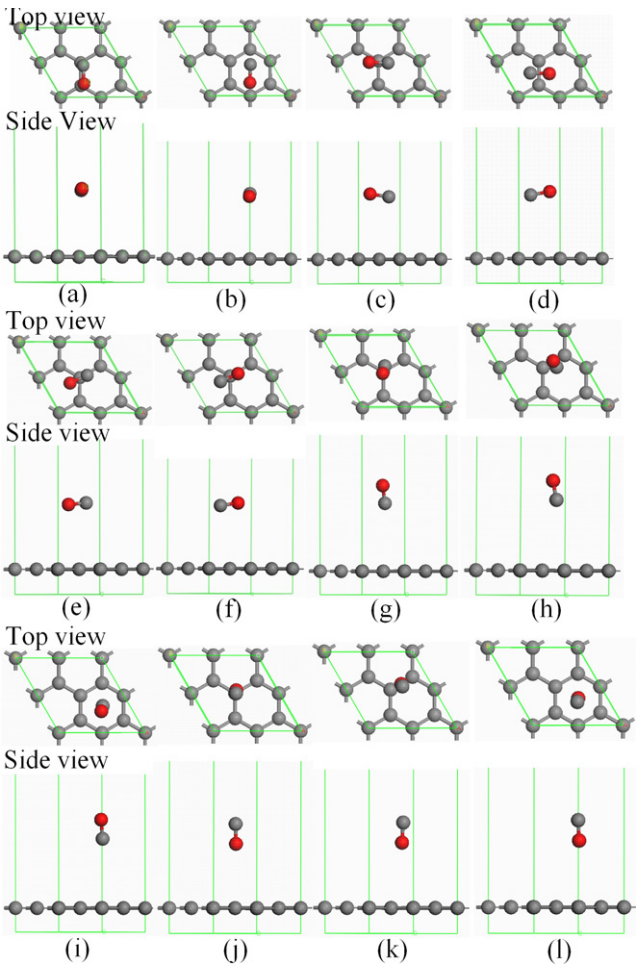

Fig. 1. Twelve available binding sites for CO adsorbed on intrinsic graphene (top and below images show the top and side view, respectively). (a) T–B–T, (b) T–H–T, (c) H–T–H, (d) H–B–H, (e) B(C atom)–T–H, (f) B(O atom)–T–H, (g) T(O atom upward), (h) B(O atom upward), (i) H(O atom upward), (j) T(C atom upward), (k) B(C atom upward), (l) H(C atom upward). T, B, and H denote top site of C atoms, bridge site of C–C bond, and hollow site of carbon hexagon, respectively. Gray, pink, and red spheres are denoted as C, Al, and O atoms, respectively. (For interpretation of the references to color in this figure legend, the reader is referred to the web version of this article.) In Figs. 2 and 3, spheres have the same meaning as that in Fig. 1.

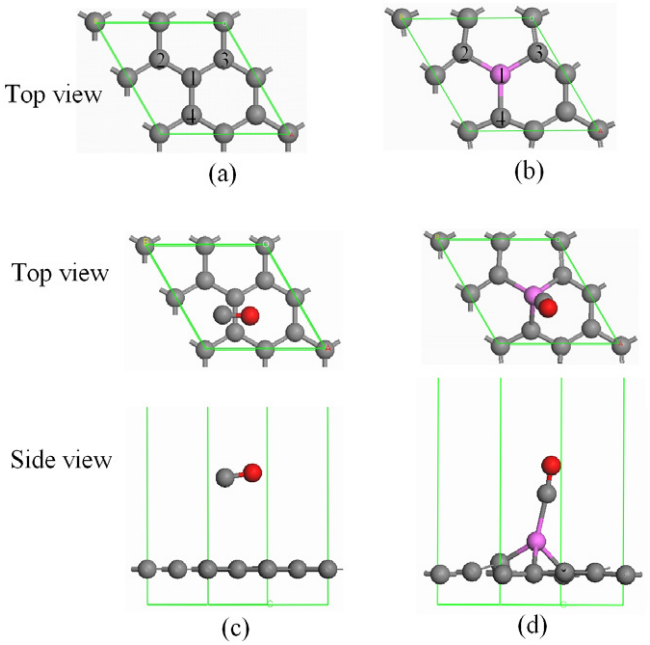

Fig. 2. Atomic configurations of intrinsic graphene and Al doped graphene before and after adsorption of CO gas molecule where one Al atom dopes in site 1, and sites 2, 3, and 4 are C atoms near the doped Al atom. (a) and (b) are the relaxed configurations of intrinsic graphene and Al doped graphene without adsorption. (c) and (d) are the preferred configurations after CO adsorption for intrinsic graphene and Al doped graphene, respectively. (For interpretation of the references to color in this figure legend, the reader is referred to the web version of this article.)

and the binding distance, d, with all possible configurations are calculated. Twelve possible binding sites for the CO adsorbed on graphene layer are considered as initial structures. After full relaxation, no distinct structural change has been found. All of the results are displayed in Table 1. It is found that adsorption configuration shown in Fig. 1f has the smallest d value and the largest E_b value among all the possible adsorption configurations. This indicates that the configuration shown in Fig. 1f is the most stable atomic arrangement with the lowest energy and the strongest interaction between CO and graphene with $E_b = 0.016$ eV and $d = 3.768$ Å which are consistent with the other simulation results of $E_b = 0.014$ eV and $d = 3.740$ Å [11]. However, in this particular adsorption configuration, the E_b is still considered too small and

Table 1
Summary of results for CO adsorption on intrinsic graphene and Al doped graphene on different adsorption sites

Initial binding configuration		Intrinsic graphene		Al doped graphene	
		E_b (eV)	d (Å)[a]	E_b (eV)	l (Å)[b]
CO//graphene	T–B–T	−0.011	3.839	−4.978	1.964
	T–H–T	−0.012	3.805	−4.973	1.968
	H–T–H	−0.014	3.826	−4.613	3.755[a]
	H–B–H	−0.009	3.857	−4.599	3.814[a]
	B(C atom)–T–H	−0.011	3.855	−4.609	3.800[a]
	B(O atom)–T–H	−0.016	3.768	−4.616	3.821[a]
CO⊥graphene	T(O upwards)	−0.007	3.938	−4.979	1.961
	B(O upwards)	−0.007	3.935	−4.978	1.964
	H(O upwards)	−0.003	3.982	−4.975	1.965
	T(C upwards)	−0.004	3.952	−4.629	3.781[a]
	B(C upwards)	−0.003	3.981	−4.607	3.783[a]
	H(C upwards)	−0.005	3.942	−4.609	3.457[a]

The meaning of T, B, and H is given in the caption of Fig. 1.
[a] Binding distance between CO gas molecule and graphene layer.
[b] Bond length of Al and C atom in CO gas molecule.

Table 2
Some structure parameters of intrinsic graphene and Al doped graphene before and after adsorption of CO molecule

System	Configuration	Bond	Bond length l (Å)	Q (e)[a]
Intrinsic graphene	Fig. 2a	C1–C2	1.420	
		C1–C3	1.420	
		C1–C4	1.420	
	Fig. 2c	C1–C2	1.420	0.003
		C1–C3	1.421	
		C1–C4	1.421	
Al doped graphene	Fig. 2b	Al1–C2	1.632	
		Al1–C3	1.632	
		Al1–C4	1.632	
	Fig. 2d	Al1–C2	1.870	0.027
		Al1–C3	1.910	
		Al1–C4	1.915	

[a] Electrons transferred from the graphene layer to CO molecule. e denotes one electronic charge.

d too large although they are the most favorable one for adsorption, reflecting that CO undergoes weak physisorption on the intrinsic graphene. This indicates that the intrinsic graphene is insensitive to CO molecules.

When one carbon atom is substituted by Al atom in the supercell, it is found that the geometric structure of the Al doped graphene changes dramatically. Fig. 2a and b represents the geometries of intrinsic and Al doped graphene after relaxation. As shown in Table 2 and Fig. 2b, the Al doping results in l elongation from $l_{C-C} = 1.420$ Å to $l_{Al-C} = 1.632$ Å. This is associated with the distortion of hexagonal structures adjacent to the larger Al atom, similar to the restructuring in Al doped SWCNTs [8].

When a CO molecule is adsorbed on the Al doped graphene, where one C atom is substituted by an Al atom in the supercell, there are also twelve available adsorption sites similar to the CO absorption in intrinsic graphene shown in Fig. 1. These are taken as initial configurations. After relaxation, the configuration in Fig. 2d has the most stable relaxed structure obtained from the initial arrangements of T–B–T, T–H–T, T(O upwards), B(O upwards) and H(O upwards) where the letters T, B and H denote the sites of atom and CO molecule center on graphene ring, and they are defined in the caption of Fig. 1. Note that in Table 1, the deviation of E_b and l_{Al-C} of the five configurations above is within the error of 1%. The adsorption of CO causes a structure change in the Al doped graphene dramatically, resulting in an expansion of l_{Al1-C2} from 1.632 Å to 1.870 Å while l_{Al1-C4} elongates from 1.632 Å to 1.915 Å. The corresponding distance between the CO molecule and Al atom in the Al doped graphene is 1.964 Å, being much shorter than 3.767 Å in the intrinsic graphene system. Moreover, the E_b of CO in the Al doped graphene system is 4.979 eV, which is over 60 times larger than that of CO in the intrinsic graphene system. Comparing with the E_b in other systems, such as $E_b = 1.280$ eV for CO adsorbed in the Al doped SWCNT systems [8], $E_b = 0.986$ eV in the B doped SWCNT systems [8] and $E_b = 0.201$ eV for CO adsorbed in B doped graphene, the Al doped graphene is energetically favorable for CO adsorption. In other words, the Al doped graphene is much more sensitive to the CO adsorption among the mentioned systems.

Furthermore, to investigate the changes of electronic structures in graphenes caused by the physi- or chemisorption of CO molecule, the net electron transfer (Q) from either the intrinsic or the Al doped graphene to the polar CO molecules is calculated by Mulliken analysis, where Q is defined as the charge variation caused by the CO absorption. As listed in Table 2, $Q = 0.027$ e in the Al doped graphene is almost one order larger than 0.003 e in the intrinsic graphene. This supports the notion that the Al doping influences the electronic properties of graphene substantially. This can also be verified by the difference of electronic densities between the intrinsic and Al doped graphenes with and without the CO adsorption as shown in Fig. 3. In the figure, the red and blue regions represent the areas of electron accumulation and the electron loss, respectively. Fig. 3a indicates that the bond in the intrinsic graphene is of covalent nature because the preferential electron accumulation sites are mainly located within the bond rather than heavily centered on a particular atom. However, the Al doping modified the electron density by inducing the different electron affinities for Al and C atoms but the whole structure remains covalent in nature (Fig. 3b). Physisorption of CO on the intrinsic graphene does not alter the electron distribution for both CO molecule and graphene, implying the weak bonding characteristics. It is discernable that electronic polarization is induced by the preferential accumulation of electrons on O in CO molecules (Fig. 3c). As distinct from the CO absorption on the intrinsic graphene, the chemisorption of CO on Al doped graphene leads to significant electron transfer from the graphene to CO molecule (Fig. 3d). In this case, the electrons not only accumulate on the O atom but also on the C atom of the molecule bond with the doped Al atom. The final position of Al atom in the chemisorbed CO–Al–graphene complex is thus a direct consequence of the maximized degree of sp^3 orbital hybridization with neighboring C atoms from both the graphene layer and CO molecule. This is evidential because the red lobes around C atoms in Fig. 3d are both pointing towards Al atom.

To further determine the effects of CO absorption on electrical conductivity, the electronic densities of state (DOSs) for both systems with and without the absorption are calculated. As shown in Fig. 4a and b, the Al doping in graphene enhances its electrical conductivity by shifting the highest DOS peak to just below the Fermi level E_f, which also leads to reduction of E_g. This indicates that the doping Al atom induces shallow acceptor states in graphene like B atom in SWCNs, thus enhancing its extrinsic conductivity [4]. When the CO molecule was adsorbed on the intrinsic and doped graphene surfaces, the total DOSs are shown in Fig. 4c and d. In the intrinsic graphene, the DOS of CO–graphene system near E_f has no distinct change, and the conductivity change is barely observable. It implies that the intrinsic graphene would not be an

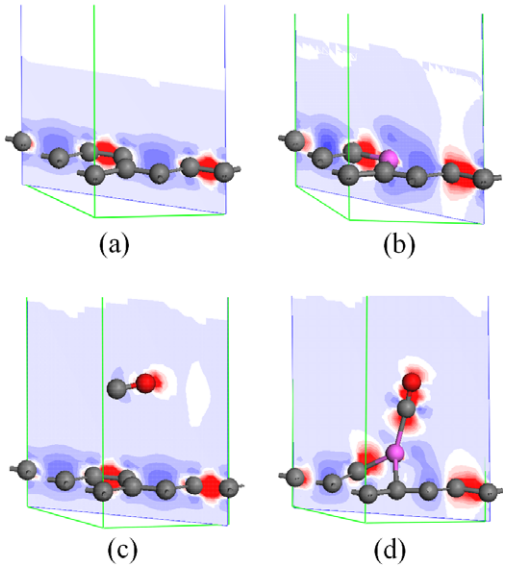

Fig. 3. Images of the electronic density difference for intrinsic graphene (a), Al doped graphene (b), CO–graphene system with preferred configuration (c), and CO–Al doped graphene system with preferred configuration (d). The red region shows the electron accumulation, while the blue region shows the electron loss. (For interpretation of the references to color in this figure legend, the reader is referred to the web version of this article.)

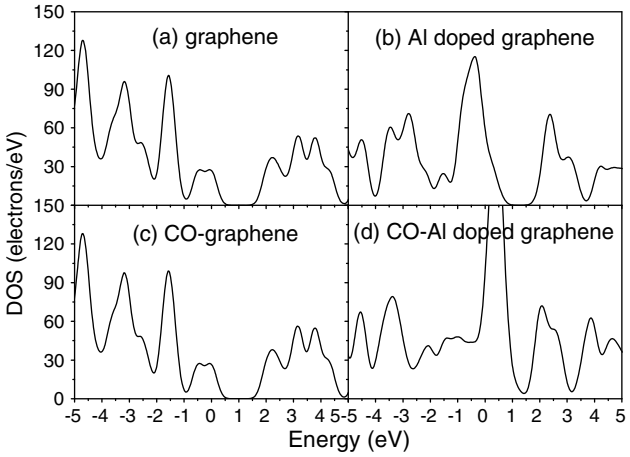

Fig. 4. Electronic density of state (DOS) of intrinsic graphene (a), Al doped graphene (b), CO–graphene system with preferred configuration (c), and CO–Al doped graphene system with preferred configuration (d).

ideal CO gas sensor. However, for the Al doped graphene with the most stable chemisorbed CO configuration (Fig. 2d), not only the highest DOS peak shifts over the E_f, but also the DOS value increases dramatically. This results in an E_g closure (Fig. 4d) where E_g of the Al doped graphene is 0.18 eV without adsorption and the E_g becomes zero with adsorption. It suggests that an extra number of shallow acceptor states is introduced when the Al doped graphene interacts with the highly polar CO molecule. As a result, the chemisorbed CO on the Al doped graphene will give rise to a large increase in the electrical conductivity of the doped graphene layer. By detecting the conductivity change of the Al doped graphene systems before and after the adsorption of CO, the presence of this toxic molecule can be detected sensitively. Therefore, the Al doped graphene is a promising sensor material for detecting CO molecules. However, desorption of CO molecule from the Al doped graphene is difficult due to the strong bonding of Al–CO [25]. This can be solved by applying an electric field F to reactivate the sensor materials [26].

In conclusion, the adsorptions of CO molecules on the intrinsic and Al doped graphenes are investigated using DFT calculation. It is found that CO molecules are only weakly adsorbed onto the intrinsic graphene with small binding energy value and large distance between the CO molecules and graphene. The electronic structure and electrical conductivity of the intrinsic graphene have a limited change caused by the adsorption of CO molecules. However, the CO molecule has strong interaction with the Al doped graphene, forming an Al–CO bond that introduces a large amount of shallow acceptor states into the system. In this case, the remarkable variation of the electrical conductivity is induced by the CO adsorption, possessing an excellent characteristic of high sensitivity for CO gas detection.

Acknowledgments

This work was financially supported by National Key Basic Research and Development Program (Grant No. 2004CB619301), '985 Project' of Jilin University and Australia Research Council Discovery Program DP0665539.

References

[1] P.T. Moseley, Meas. Sci. Technol. 8 (1997) 223.
[2] J. Kong, N.R. Franklin, C. Zhou, M.G. Chapline, S. Peng, K. Cho, H. Dai, Science 287 (2000) 622.
[3] P.G. Collins, K. Bradley, M. Ishigami, A. Zettl, Science 287 (2000) 1801.
[4] S. Peng, K. Cho, Nano Lett. 3 (2003) 513.
[5] J. Kong, M.G. Chapline, H. Dai, Adv. Mater. 13 (2001) 1384.
[6] B.Y. Wei, M.C. Hsu, P.G. Su, H.M. Lin, R.J. Wu, H.J. Lai, Sens. Actuators, B 101 (2004) 81.
[7] Q. Zhao, M.B. Nardelli, W. Lu, J. Bernholc, Nano Lett. 5 (2005) 847.
[8] R. Wang, D. Zhang, W. Sun, Z. Han, C. Liu, J. Mol. Struc.: Theochem. 806 (2007) 93.
[9] Y.M. Zhang, D.J. Zhang, C.B. Liu, J. Phys. Chem. B 110 (2006) 4671.
[10] F. Schedin, A.K. Geim, S.V. Morozov, E.W. Hill, P. Blake, M.I. Katasnelson, K.S. Novoselov, Nat. Mater. 6 (2007) 652.
[11] O. Leenaerts, B. Partoens, F.M. Peeters, Phys. Rev. B 77 (2008) 125416.
[12] T.O. Wehling, K.S. Novoselov, S.V. Morozov, E.E. Vdovin, M.I. Katsnelson, A.K. Geim, A.I. Lichtenstein, Nano Lett. 8 (2008) 173.
[13] A.K. Geim, K.S. Novoselov, Nat. Mater. 6 (2007) 183.
[14] K.S. Novoselov et al., Nature 438 (2005) 197.
[15] Y. Zhang, J.W. Tan, H.L. Stormer, P. Kim, Nature 438 (2005) 201.
[16] M.S. Dresselhaus, G. Dresselhaus, Adv. Phys. 51 (2002) 1.
[17] P. Dutta, P.M. Horn, Rev. Mod. Phys. 53 (1981) 497.
[18] B. Delley, J. Chem. Phys. 92 (1990) 508.
[19] B. Delley, J. Chem. Phys. 113 (2000) 7756.
[20] L. Jeloaica, V. Sidis, Chem. Phys. Lett. 300 (1999) 157.
[21] A. Lugo-Solis, I. Vasiliev, Phys. Rev. B 76 (2007) 235431.
[22] B. Hammer, L.B. Hansen, J.K. Nørskov, Phys. Rev. B 59 (1999) 7413.
[23] B. Delley, J. Chem. Phys. 66 (2002) 155125.
[24] D.R. Lide, CRC Handbook of Chemistry and Physics, 81st edn., CRC Press, Boca Raton, FL, 2000.
[25] S. Peng, K. Cho, P. Qi, H. Dai, Chem. Phys. Lett. 387 (2004) 271.
[26] M.P. Hyman, J.W. Medlin, J. Phys. Chem. B 109 (2005) 6304.